General Disclaimer

One or more of the Following Statements may affect this Document

- This document has been reproduced from the best copy furnished by the organizational source. It is being released in the interest of making available as much information as possible.

- This document may contain data, which exceeds the sheet parameters. It was furnished in this condition by the organizational source and is the best copy available.

- This document may contain tone-on-tone or color graphs, charts and/or pictures, which have been reproduced in black and white.

- This document is paginated as submitted by the original source.

- Portions of this document are not fully legible due to the historical nature of some of the material. However, it is the best reproduction available from the original submission.

Far Infrared Maps of the Ridge Between OMC-1 and OMC-2

Jocelyn Keene[a,b], J. Smith[c], D. A. Harper[b,c] R. H. Hildebrand[a,b,d],

and S. E. Whitcomb[a,d]

The University of Chicago
Chicago, Illinois 60637

March 1979 Draft

a) Enrico Fermi Institute

b) Department of Astronomy and Astrophysics

c) Yerkes Observatory

d) Department of Physics

ABSTRACT

Dust continuum emission from a 6' x 20' region surrounding OMC-1 and OMC-2 has been mapped at 55 and 125 μm with 4' resolution. The dominant features of the maps are a strong peak at OMC-1 and a ridge of lower surface brightness between OMC-1 and OMC-2. Along the ridge the infrared flux densities and the color temperatures decrease smoothly from OMC-1 to OMC-2.

OMC-1 is heated primarily by several optical and infrared stars situated within or just at the boundary of the cloud. At the region of minimum column density between OMC-1 and OMC-2 the nearby B0.5 V star NU Ori may contribute significantly to the dust heating. Near OMC-2 dust column densities are large enough so that, in addition to the OMC-2 infrared cluster, the nonlocal infrared sources associated with OMC-1 and NU Ori can contribute to the heating.

I. INTRODUCTION

In this paper we present 55 and 125 μm maps, at 4' resolution, of a 6' x 20' region in Orion containing the molecular clouds OMC-1 and OMC-2. A 400 μm map of approximately the same region by Smith et al. (1979b) shows a ridge of emission extending from OMC-1 through OMC-2 and continuing several arcmin to the north. Analysis of the 400 μm map and of molecular line maps (Kutner et al. 1976) shows that the condensations associated with OMC-1 and OMC-2 are of comparable mass, $\sim 10^3 M_\odot$, and size, $\sim$2 pc. Higher resolution studies (Harper 1974, Werner et al. 1976, Thronson et al. 1978) have concentrated on the immediate vicinity of the OMC-1 and OMC-2 infrared clusters. The emphasis of the present work has been to study the large scale flux and temperature distributions by simultaneous mapping at two wavelengths and to use the results with other available data to understand the sources of dust heating in this region.

II. OBSERVATIONS

The observations presented here were made with the 0.3 m, f/7.5 telescope of the NASA Lear Jet Observatory during ten flights in February and March 1978. The photometer (Moseley 1979) provided simultaneous measurements in two broad passbands (42 μm-70 μm and 88 μm-320 μm at half power) with mean wavelengths near 55 μm and 125 μm. The beam diameters (FWHM) were 4'. The reference beam spacing was 15', oriented approximately east-west.

The maps shown in Figure 1 were constructed from photometry of individual points; signals for each point were obtained by repetitive beam switching at fixed positions. Because of the large beam spacing, no corrections were made for possible flux in the reference beams. Sampling intervals were ≤1.5 along the ridge joining OMC-1 and OMC-2, and 3' over the remainder of the map. The positional uncertainty in the 125 μm map is ±0.5 ; the two beam centers are coincident within 0.7'. The OMC-1 peak was measured periodically to calibrate the signals and monitor atmospheric extinction (<8% at 55 μm; <20% at 125 μm). Flux densities were derived from the observed signals as described by Loewenstein et al. (1977), using an assumed spectrum of the form $\nu B(\nu,T)$ where $\pi B(\nu,T)$ is the Planck function. For a 4' diameter beam centered on OMC-1, we assume flux densities of 4×10^5 Jy and 2×10^5 Jy at 55 μm and 125 μm respectively (Thronson et al. 1978, Harper 1974) corresponding to a temperature of 60K. We assume a peak flux of 3×10^{-8} Wm^{-2} for the 4' diameter region (Thronson et al. 1978) which implies a luminosity of $2.5 \times 10^5 L_\odot$ for an assumed distance of 500 pc.

The statistical errors (1σ) at points displaced more than 3' from the OMC-1 peak are typically 0.5% of the peak flux (i.e., 2000 Jy at 55 μm and 1000 Jy at 125 μm). The uncertainties due to spectral corrections are comparable to the statistical errors over most of the map. The absolute calibration has an estimated error of ∿20%.

III. RESULTS

Maps of 55 μm and 125 μm surface brightness are presented in Figures 1a and 1b. At both wavelengths, a strong maximum at OMC-1 dominates the map. At lower levles (1-10% of the peak surface brightness) the principal feature is a ridge of emission approximately 12' NS x 6'EW between OMC-1 and OMC-2. At the temperatures derived for the mapped region (∿40-65K, see below) a map of total flux is essentially equivalent to the 55 μm map shown in Fig. 1a. Only in the hottest regions near OMC-1 (T>75K) does the total flux map differ from the 55 μm map by >30%. Integration over the maps yields total flux densities of $F(55\ \mu m) = 7 \times 10^5$ Jy and $F(125\ \mu m) = 4 \times 10^5$ Jy, nearly twice that observed at OMC-1 with the 4' beam. The total infrared flux from the mapped area implies a luminosity $4.5 \times 10^5 L_\odot$ of which 90% is emitted near OMC-1 (south of -5° 20'). The remaining 10% ($4 \times 10^4 L_\odot$) comes from the region 4' north of OMC-1 comprising ∿1/2 of the total area.

The present observations do not show the compact sources found with higher resolution observations. In addition to the 6' source centered on OMC-1, there is a compact source (1' in diameter) associated with the OMC-1 infrared cluster (Harper 1974, Fazio et al. 1974, Werner et al. 1976). Similarly, 0.5' observations show a compact source centered on the OMC-2 infrared cluster (Thronson et al. 1978). With a measured total flux of $2 \times 10^{-10} Wm^{-2}$ (Thronson et al. 1978) this source would produce only a 40% increase above the mean ridge flux observed with a 4' beam, an amount too small to appear on our maps. With 1' resolution, Harper (1974) and Fazio et al. (1974) have observed a 1' - 3' diameter, low contrast source associated with NU Ori, the exciting star for M43. Our observed flux at

that point, $2 \times 10^{-9} Wm^{-2}$ corresponding to a luminosity of $1.5 \times 10^{4} L_{\odot}$, is an upper limit to the flux from a discrete source at that point. It is evident that our results reflect large scale heating and energetics rather than the local effects of individual stellar sources.

Figure 2 shows in detail the 55 and 125 μm flux densities measured along the ridge through OMC-1 and OMC-2 (4' beam) and, for comparison, the corresponding 400 μm flux densities measured by Smith et al. (1979b; 3' beam). The shift of the continuum emission toward longer wavelengths as one moves from OMC-1 to OMC-2 is obvious; the ratio of the flux density at OMC-1 to that at OMC-2 decreases from ∿60 at 55 μm to ∿10 at 400 μm.

In Figure 1c we present a map showing color temperatures which are derived assuming that the flux is due to optically thin thermal emission from dust with an emissivity proportional to ν^n where n = 1. Taking this value of n one obtains a good fit to the measured spectrum at OMC-1 between 30 μm and 150 μm (Thronson et al. 1978). A stronger dependence of emissivity on frequency ($n \approx 2$) is required at longer wavelengths to fit the 400 μm flux density measured by Smith et al. (1979b). The values derived for temperature and optical depth depend on the emissivity. However, the relative values of these quantities are insensitive to the choice of n for points within the mapped region.

The color temperature map in Figure 1c shows no local extrema. A prominent feature of the figure is the shift in direction of the temperature gradients between the northern and southern regions. In the region north of NU Ori containing OMC-2, the temperatures decrease from south to north; in the vicinity of OMC-1 they decrease from west to east.

In Figure 3 we show scans of total infrared flux, 55 μm/125 μm color temperature, and 125 μm optical depth along the ridge between OMC-1 and OMC-2. The color temperature has a value of ∿60K near OMC-1 and falls to ∿40K near OMC-2, with a shoulder near the declination of NU Ori ($\Delta\delta \approx +7'$). The 125 μm optical depths are derived from the flux densities shown in Figure 2 and the color temperaures in Figure 3. Like the submillimeter optical depths derived for the ridge by Smith et al. (1979b), the 125 μm optical depth has a minimum ∿8' north of OMC-1, in the vicinity of NU Ori.

A comparison of Figures 1a and 1b with the $^{13}CO(J=1\rightarrow0)$ molecular line map (Kutner et al. 1976) shows that the width of the ridge is smaller for the dust continuum flux densities than for the ^{13}CO line temperatures. Profiles ∿10' north of OMC-1, for example, show a full width at half maximum of ∿5'-6' for the dust emission and ∿10' for the ^{13}CO line temperature.

IV. DISCUSSION

Based on their 400 μm observations and the CO observations of Kutner et al. (1976), Smith et al. (1979b) have concluded that the dust responsible for the submillimeter radiation is associated with two separate condensations of comparable mass ($10^3 M_\odot$), size (2 pc), and optical depth. The southern condensation is centered on OMC-1; the northern ∿6' north of OMC-2.

Because of the similarity of the 55 and 125 μm maps to the 400 μm map, particularly the presence and size of the ridge, and the correlation between the 125 μm and 400 μm optical depths, we shall assume that the dust responsible for the 55 and 125 μm emission is also associated with the molecular clouds and that it may be the same dust responsible for the 400 μm emission. With these assumptions we shall discuss the large scale energetics of the region.

a) OMC-1 Region

In the vicinity of OMC-1 south of -5° 20', our observed luminosity, $4 \times 10^5 L_\odot$, can be accounted for by the combined luminosities of the OB stars in the Trapezium and θ^2 Ori ($L_\star = 3 \times 10^5 L_\odot$, $A_V \sim 2$ mag., Smith et al. 1979a) and the OMC-1 infrared cluster ($L_\star \gtrsim 1 \times 10^5 L_\odot$, Werner et al. 1976). The color temperatures to the west of OMC-1 show the effect of dust associated with M42; the increase of color temperature with increasing distance westward from the Trapezium indicates that the column density of warm dust associated with the HII region decreases less rapidly than that of the cooler dust associated with the molecular cloud. Radio continuum observations (Goss and Shaver 1970) also show the greater extent of the HII region to the west. Higher resolution far-infrared observations (Werner et al. 1976) show details not resolved in the present data. They show, for example, that the infrared

cluster dominiates the heating within a 1' diameter region, and that the Trapezium is responsible for powering an ionization front ∿2' to the southeast.

b) Region of minimum column density

We must account for an observed luminosity of ∿2 x $10^4 L_\odot$ in the region of minimum column density between OMC-1 and OMC-2 (∿8' north of OMC-1); the exact luminosity is uncertain due to the large beam used for the observations and the proximity of the very bright 6' wide source at OMC-1. Two sources to consider are NU Ori and OMC-1.

The luminosity (2 x $10^4 L_\odot$), extinction (2.4 mag., Smith et al. 1979a) and position (∿2' east of the ridge) of NU Ori suggest that it may be an important source for heating the dust near the ridge. The observed constancy of the ridge temperature north of OMC-1 also suggests that local heating of the ridge persists to near the declination of NU Ori. The diameter of M43 observed at 5 GHz (3.3', Goss and Shaver 1970) shows that the stellar flux from NU Ori extends ∿2', the perpendicular distance to the center of the ridge. That flux will be absorbed much more efficiently than the far-infrared flux from OMC-1, and hence will be the dominant heat source wherever the NU Ori flux is a substantial fraction of the OMC-1 flux. At the center of the ridge 7' north of OMC-1 the incident flux from NU Ori could be ∿60% of that from OMC-1. On the other hand, the luminosity observed with a 4' beam exceeds the possible contribution of NU Ori by at least a factor of 2, implying that OMC-1 must also make a substantial contribution of the overall heating. The relative contributions of the two sources depends on the geometry of the ridge.

c) OMC-2 Region

At OMC-2 there may be significant contributions to the dust heating from at least three sources: the OMC-2 infrared cluster, NU Ori, and OMC-1.

The total far-infrared luminosity observed with the 4' beam is 4000 $L_\odot$. The infrared cluster is imbedded in the edge of the northern condensation; the dense surrounding material should be efficient in converting the primary radiation into the far-infrared. However, with a luminosity of only 600 $L_\odot$ (Thronson et al. 1978; 0.83' beam) the infrared cluster can contribute no more than 15% of the observed flux. The steep north-south temperature gradient suggests that heating by the southern sources (NU Ori and OMC-1) is important. For a 4' diameter region centered on OMC-2, the optical flux from NU Ori can contribute at most $\sim$600 $L_\odot$. The flux from OMC-1 is $\sim$5 times larger. The total flux from these three sources is sufficient to account for the observed total luminosity at OMC-2 but only if that region is nearly opaque to the infrared radiation from OMC-1 or if the total radiation from the OMC-2 infrared cluster is substantially greater than has been observed with the 0.83' beam used by Thronson et al. (1978).

V. CONCLUSIONS

We have mapped a 6' x 20' region including OMC-1 and OMC-2 with a resolution of 4' at 55 μm and 125 μm and have derived far-infrared color temperatures for the mapped region. The OMC-1 source with a size of 6' FWHM emits 90% of the observed luminosity. A ridge of lower surface brightness extends from OMC-1 to OMC-2. Temperatures along the ridge decline from ∿60K near OMC-1 to ∿40K at OMC-2. South of NU Ori the temperature gradient is predominately east-west; further north, in the region of OMC-2, the gradient is north-south.

In the region of minimum column density between OMC-1 and OMC-2, the present observations show evidence for local heating by the optical flux from NU Ori and by the infrared flux from OMC-1. In the region of OMC-2 the known sources, the OMC-2 infrared cluster, OMC-1 and NU Ori, are barely sufficient to account for the observed luminosity unless the opacity is greater or the cluster more luminous that expected.

ACKNOWLEDGEMENTS

We wish to thank J. Fischer, and R. F. Loewenstein for assistance in the observations, and S. H. Moseley and R. Pernic for assistance with instrumentation. We appreciate the support and assistance provided by the staff of the Medium Altitude Missions Branch of Ames Research Center. J. K. and S. E. W. wish to acknowledge support from the Fannie and John Hertz Foundation. This work as supported by the National Aeronautics and Space Administration under grant No. NSG-2261.

REFERENCES

Bohlin, R. C., Savage, B. D., and Drake, J. F. (1978). Astrophys. J. 224, 132.

Fazio, G. G., Kleinmann, D. E., Noyes, R. W., Wright, E. L., Zeilik, M., and Low, F. J. (1974). Astrophys. J.(Letters) 192, L23.

Gatley, I., Becklin, E. E., Matthews, K., Neugebauer, G., Penston, M. V., and Scoville, N. (1974). Astrophys. J. (Letters) 191, L121.

Goss, W. M., and Shaver, P. A. (1970). Australian J. Phys., Suppl. No. 14, p.1.

Harper, D. A. (1974). Astrophys. J. 192, 557.

Kutner, M. L., Evans, N. J., and Tucker, K. D. (1976). Astrophys. J. 209, 452.

Loewenstein, R. F., Harper, D. A., Moseley, S. H., Telesco, C. M., Thronson, H. A., Hildebrand, R. H., Whitcomb, S. E., Winston, R., and Stiening, R. F. (1977), Icarus 31, 315.

Moseley, S. H. (1979). Ph.D. Dissertation, University of Chicago.

Smith, J., Hackwell, J. A., and Gehrz, R. D. (1979a). In preparation.

Smith, J., Lynch, D. K., Cudaback, D., and Werner, M. W. (1979b). In preparation.

Thronson, H. A., Harper, D. A., Keene, J., Loewenstein, R. F., Moseley, S. H., and Telesco, C. M. (1978). Astron. J. 83, 492.

Werner, M. W., Gatley, I., Harper, D. A., Becklin, E. E., Loewenstein, R. F., Telesco, C. M., and Thronson, H. A. (1976). Astrophys. J. 204, 420.

FIGURE LEGENDS

Figure 1 Far infrared maps of the region between OMC-1 and OMC-2. Contour maps of a) 55 μm and b) 125 μm flux density, normalized to a peak value of 100. c) Contour map of color temperatures derived assuming spectra of the form $\nu B(\nu,T)$. The position of OMC-1 (the Kleinmann-Low Nebula) is marked by a cross; the position of OMC-2/IRS-4 (Gatley et al. 1974) is marked by a triangle. The filled circles mark the positions of the stars NU Ori, θ^2 A and B, and the Trapezium. The dashed line in Fig. 1a indicates the location of the one-dimensional scans shown in Figures 2 and 3.

Figure 2 Flux densities at 55 μm and 125 μm (this work) and at 400 μm (Smith et al. 1979) along the ridge between OMC-1 and OMC-2 (see dashed line, Fig. 1a). $\Delta\delta$ = displacement in declination from -5° 24.'7, the position of OMC-1 (the Kleinmann-Low Nebula). For the 4' beam of these observations, we assume flux densities of 4×10^5 Jy at 55 μm and 2×10^5 Jy at 125 μm for $\Delta\delta = 0$. The statistical errors are in the range 12-25% for the four northernmost 55 μm points and $\leq$10% for all other points.

Figure 3 Scans of total infrared flux,55 μm/125 μm color temperature, and 125 μm optical depth along the ridge between OMC-1 and OMC-2 (see dashed line, Fig. 1a). $\Delta\delta$ = displacement in declination from 15° 24.'7. For the 4' diameter beam of these observations we assume a flux of 3×10^{-8} Wm^{-2} and a 55 μm/125 μm colar temperature of 60K at $\Delta\delta = 0$. Statistical errors in flux are shown wherever the error bars are larger than the points. The total errors shown

for the color temperatures include statistical errors in flux density and the (larger) systematic errors due to possible misalignment of the 55 μm and 125 μm beams with respect to each other. The errors in optical depth include the effects of temperature errors (asymmetrical; dominant for most points), and of statistical errors in flux density (symmetrical; dominant for northernmost points).

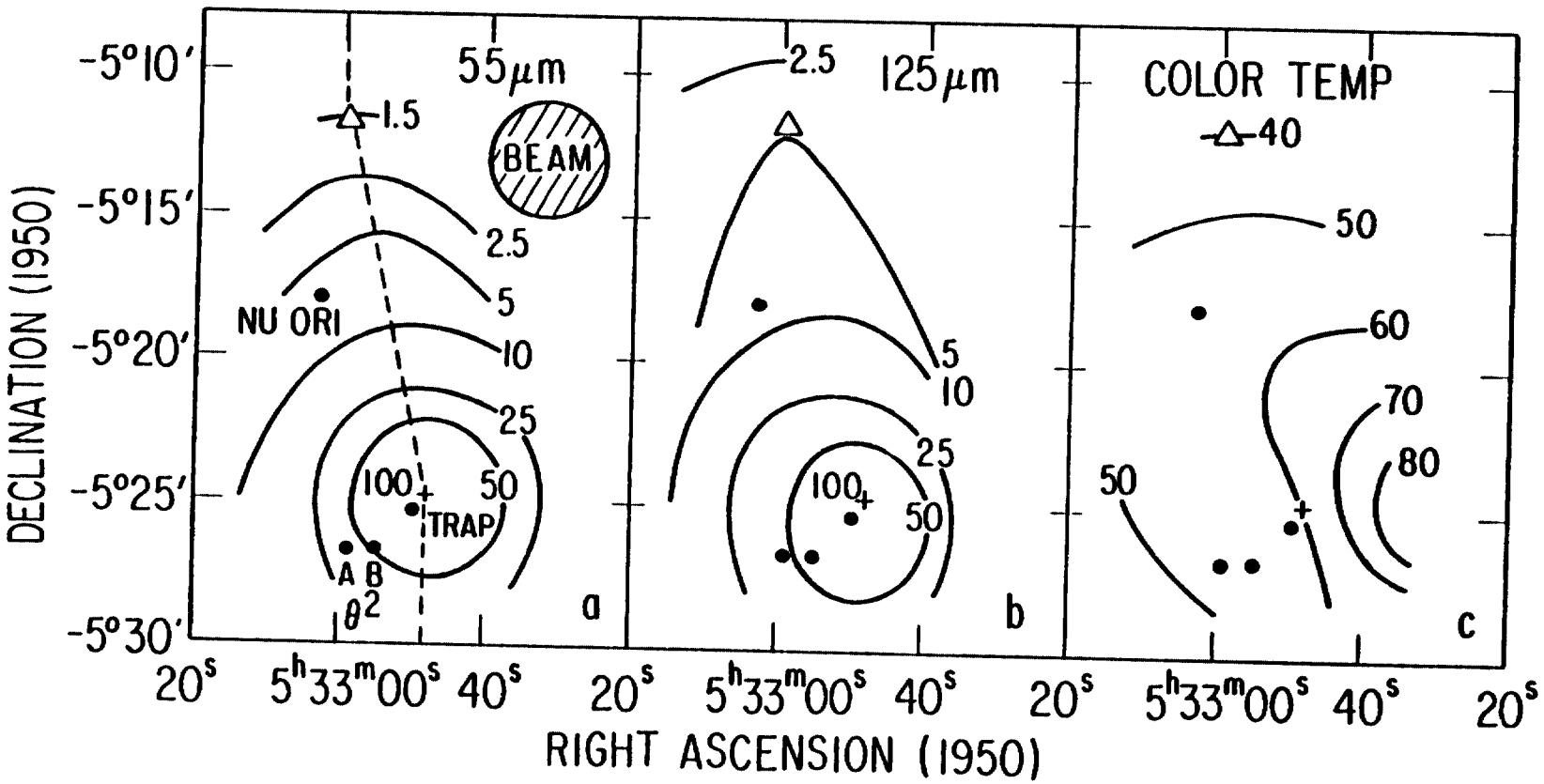
55μm
125μm
COLOR TEMP
BEAM
1.5
2.5
5
10
25
50
100
NU ORI
TRAP
A B
θ2
a
b
c
40
60
70
80
-5°10'
-5°15'
-5°20'
-5°25'
-5°30'
DECLINATION (1950)
20s
5h33m00s
40s
RIGHT ASCENSION (1950)

Fig.1

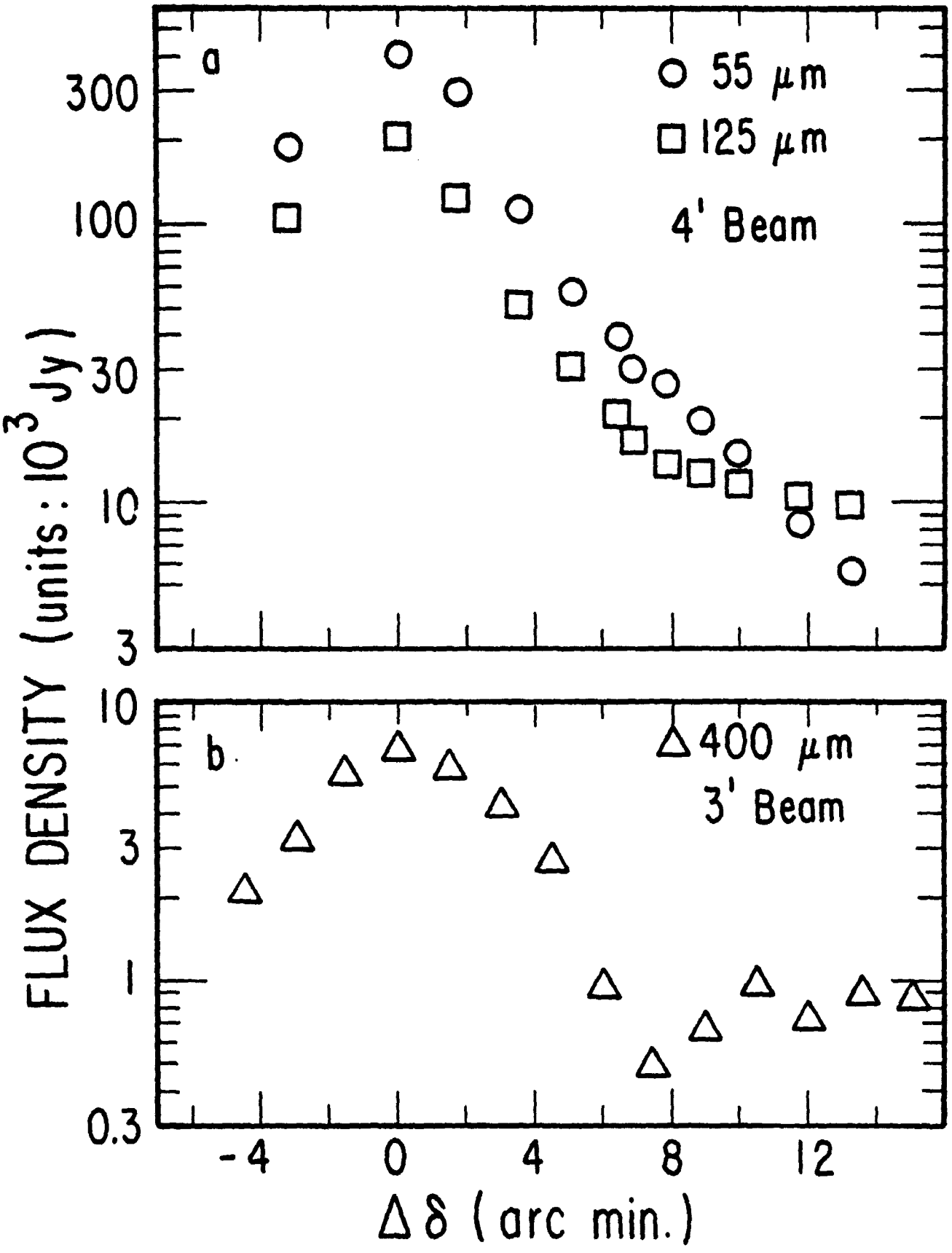
a
55 μm
125 μm
4' Beam
300
100
30
10
3
b
400 μm
3' Beam
10
3
1
0.3
FLUX DENSITY (units: 10^3 Jy)
-4
0
4
8
12
Δδ (arc min.)

Fig.2

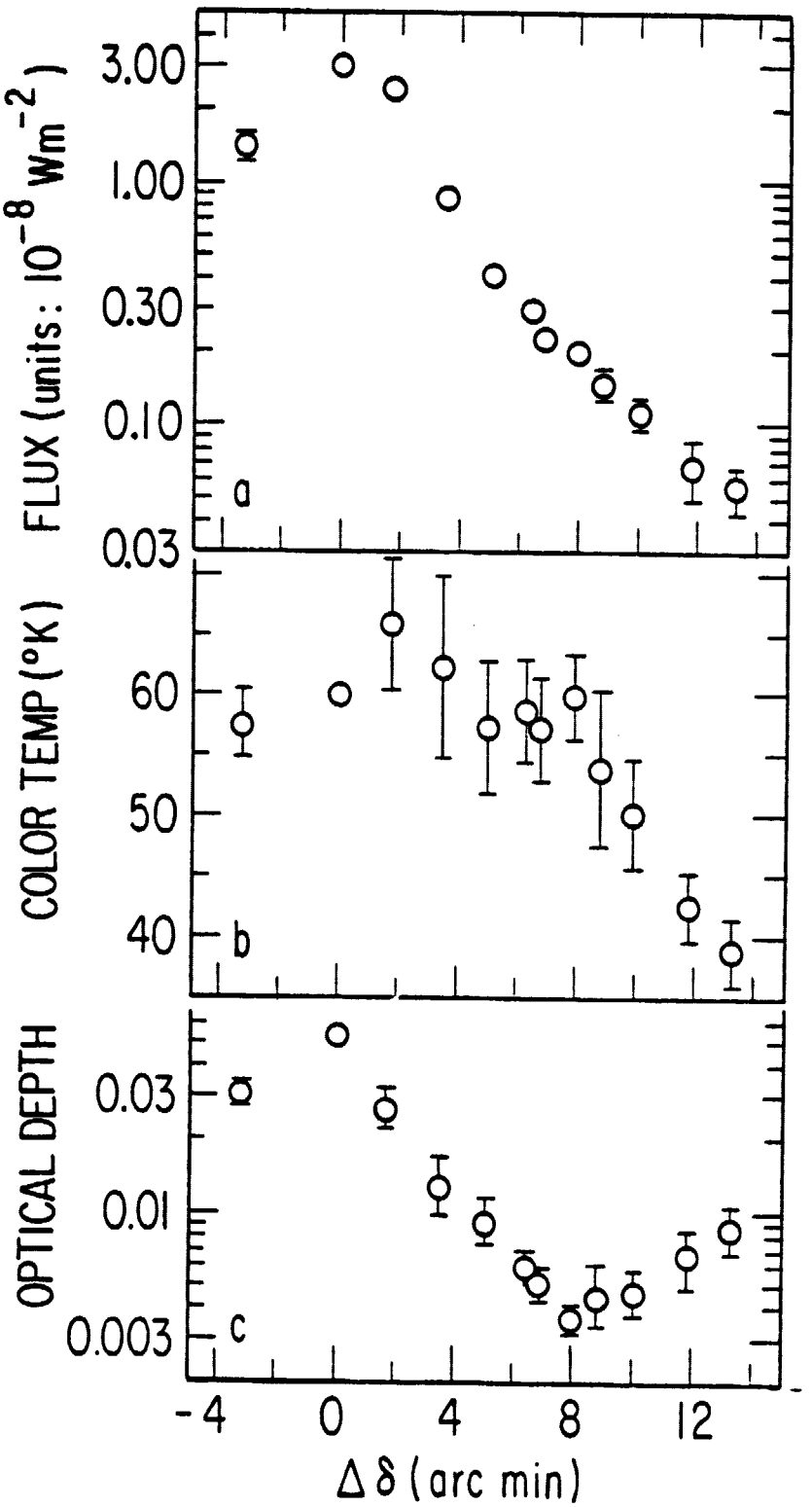
FLUX (units: 10^{-8} Wm^{-2})
3.00
1.00
0.30
0.10
0.03
a
COLOR TEMP (°K)
60
50
40
b
OPTICAL DEPTH
0.03
0.01
0.003
c
-4
0
4
8
12
Δδ (arc min)

Fig. 3